The Slitted Decouple Design for Metallic Item Detection in UHF RFID Systems

Zhonghao HU [1], Peter Cole [2]

The University of Adelaide
Adelaide, Australia
[1]nathanhu@eleceng.adelaide.edu.au
[2]cole@eleceng.adelaide.edu.au

***Abstract*— Recently, an electromagnetic radiation decoupler with significant advantages (low profile and simple structure) was proposed for metallic item detection in UHF RFID systems. In this paper the decoupler is investigated by simulation and experiment. Based on the simulation, some new design principles, different from the original principles of the inventors, aimed at optimizing the performance of the decoupler, are proposed. These new design principles are verified by measurement.**

I. Introduction

RFID is a type of automatic identification technology making use of radio waves. UHF RFID systems are RFID systems operating in the ultra high frequency band, which is around 1GHz for RFID applications. UHF RFID systems have been widely used in many areas such as in supply chains, in airport luggage management and in animal tracking [1]. However, the electromagnetic boundary condition that there is no tangential electric field component on a metal surface brings some obstacles to detect metallic items by RFID tags, as most tag antenna's excitation significantly depends on a tangential electric field. Hence, solutions for metallic item identification must be found. Among existing solutions, the earliest is to insert a one quarter wavelength spacing between an antenna and a metallic item. However, one quarter wavelength (75mm around 1GHz) makes the whole structure suffer from being bulky and easily damaged. Sung et al. [2] shortened the space between the antenna and the metal by using high permittivity materials such as BaTiO3(BT). They achieved a thickness of less than 4mm at 2GHz. However, manufacturing these high permittivity materials at a desired value of dielectric constant is complicated. Numerous procedures such as controlling sintering temperature, pressure, and the ratio of composite materials are involved. Recently, several kinds of artificial magnetic conductor (AMC) have been proposed to solve the antenna on metal problem. The reflection coefficient of AMC is +1 instead of the -1 which occurs on a metal surface [3] [4]. An AMC will be placed between an antenna and a metallic item. With the AMC, the antenna will have better radiation performance than the antenna without the AMC and placed on the metallic item directly. However, once these AMCs are designed for frequencies around 1GHz, they are either structurally complicated [3] or too thick to be applicable [4]. A new AMC named Electromagnetic Radiation Decoupler with significant advantages was invented by Brown et al. [5] to provide a low profile and simple structure solution for metallic item detection in UHF RFID systems. However, the inventors did not give adequate explanation of their invention. This paper aims to give this invention an explanation by typical electromagnetic theory, and based on the explanation, some new principles, different from the original ones proposed by the inventors [5], are made in designing this decoupler. Ansoft HFSS is used here to provide the simulation results and some experiments on the decoupler are also made to verify the design principles proposed by the authors of this paper.

II. Introduction to Electromagnetic Radiation Decoupler

The electromagnetic radiation decoupler proposed in [5] with a metallic item underneath and an RFID tag above is shown in Figure 1, and a rectangular (x, y, z) coordinate system is defined in Figure 1 to provide a basis for the further discussion. The decoupler is composed of two separated patches with a slit in the middle, a dielectric layer, and a ground plane shared by the two patches. Therefore, in the following description, we will call the electromagnetic radiation decoupler a slitted decoupler. The dimensional parameters contained in this model are the length and width (W and L) of each patch, the thickness (h) of the dielectric layer and the width (s) of the slit, and the distance D_z between the tag and the decoupler. The tag on the decoupler is expected to have longer reading range than when it is placed above the metallic item directly. The whole structure (tag with decoupler) is very thin (less than 8mm).

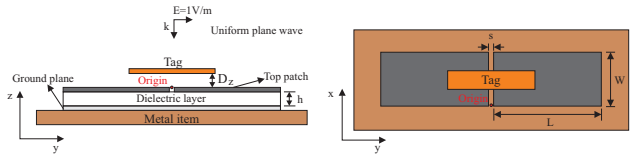

(a) Side view (b) Top view

Fig. 1. Slitted decoupler structure illustration. A tag is placed above the slitted decoupler in a distance D_z. Below the decoupler, can be seen the metal item.

Some design principles for the slitted decoupler, proposed in [5], are now listed.

- *Patch Length L*

$$L \simeq \frac{\lambda_0}{2\sqrt{\epsilon_r}} N \quad (1)$$

where λ_0 is the wavelength in the free space, ϵ_r is the relative permittivity of the sandwiched dielectric material. N is an integer. The fundamental resonant frequency is obtained when $N = 1$.

- *Patch Width W*
  The patch width may be determined by the dimension of the selected RF tag. Commonly, the patch width is 4 to 5 times that of a tag on the slitted decoupler. A reduction in patch width is stated in [5] to diminish the read range of the tag on it.
- *Thickness h*
  The thickness of the dielectric material is stated in [5] to preferably less than a few $\lambda_0/1000$.
- *Slit Width s*
  The slit width is preferably less than $\lambda_0/100$.
- *The distance D_z between a tag and slitted decoupler*
  The distance is proposed to be a few hundred micrometers.
- *Dielectric material*
  The dielectric core can be one of the commonly used dielectric materials such as polystyrene, BOPP (Biaxially oriented polypropylene film) or polycarbonate. Material with low loss is preferable.

An example of the slitted decoupler constructed according to the design principles given above and intended to be resonant at 923MHz was simulated in HFSS. Some parameters of this device are listed below. The slitted decoupler is excited by an incident uniform wave propagating as shown in Figure 1(a) towards the decoupler.

$$\lambda_r = \frac{\lambda_0}{\sqrt{\epsilon_r}}, \epsilon_r = 3.2$$
$$L = 90.5\text{mm} \simeq \frac{\lambda_r}{2}, W = 70\text{mm}$$
$$s = 0.5\text{mm} < \frac{\lambda_r}{360}, h = 1\text{mm} < \frac{\lambda_r}{180}$$

The dielectric loss tangent is 0.003. The dielectric material used here is polyester.

It is found in the simulation that there is a strong y-directed electric field in the slit. This field is quite different from that which occurs when the incident field is normally incident on metal. Moreover, the peak value of the strong y-directed electric fields attenuates sharply as we move away from the slit along either the z or y direction, as is shown in Figure 2. As a result, once the decoupler is excited by the incident wave, the slit can be understood as a power source which can generate a strong y-directed electric fields and this y-directed electric fields will excite the tag antenna on it. In terms of the distance between the tag and the decoupler, it seems to be flexible between a few hundred micrometers to a few millimeters, since with the increase of z, although the peak value of the y-directed electric field drops dramatically as shown in Figure 2(a), the relatively large y-directed electric field component (>2V/m) seems to spread over a large area along y-axis.

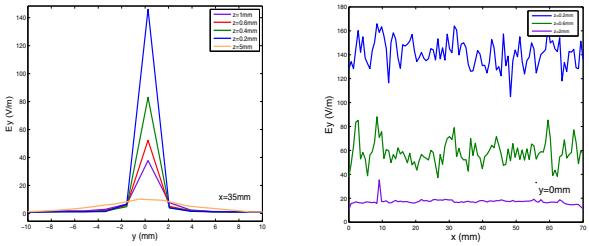

(a) Along y axis (b) Along x axis

Fig. 2. The magnitude of y-directed electric field variation along the y and x axis at various heights. E_y is the magnitude of the r.m.s. phasors of the y-directed electric fields. x, y, and z are the coordinates of the observing point in the rectangular coordinate system built in Figure 1.

The structure of the slitted decoupler inevitably makes people associate it with a pair of rectangular patch antennas. The slitted decoupler is similar to a patch antenna array which contains two rectangular cells separated by a short distance. In order to understand the operating scheme of this decoupler, it is assumed that the slitted decoupler has resonance properties similar to those of the rectangular patch antennas, so use can be made of knowledge of patch antenna properties. Although the excitation modes between the decoupler and patch antenna are very different, (one is passive radiating element which is powered by an incident wave, the other one is a driven antenna), this assumption is still reasonable by reciprocity theory. Particularly, as introduced above, the high y-directed electric fields in the slit is the power source to excite the tag on it, hence, one of the main goals in designing a well-performing decoupler is to obtain this high y-directed electric field in the slit and the y-directed electric fields in the slit of the decoupler actually are corresponded to the y-directed electric fields on the edge of rectangular patch antenna. Hence, to investigate which factors play a significant role in determining the tangential electric fields on the patch antenna edge is the task of next section.

III. Rectangular Patch Antenna Analysis

Rectangular patch antennas have been widely used in recent years due to their low profile, low cost and easy fabrication into linear or planar arrays. The structure of a simple rectangular patch antenna without excitation is shown in Figure 3. As we can see, the patch antenna is composed of three layers which are a top patch, a ground plane and a sandwiched dielectric layer. Usually, the ground plane is much bigger than the top patch.

The description at the end of Section II suggests that to design a good decoupler one should start with an understanding of a rectangular patch antenna, especially how to get the high y-directed electric fields on the edge of rectangular patch antenna. The y-directed electric fields on the edge of patch antenna are caused by fringing fields, which have been shown in Figure 3(a) and the magnitude of the y-directed electric fields and fringing fields on the patch edge significantly depend on the resistance on the patch edge as shown in the cavity

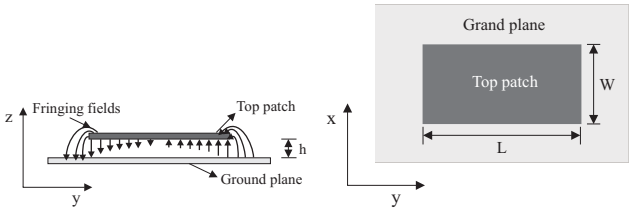

(a) Side view (b) Top view

Fig. 3. The structure of a simple rectangular patch antenna without excitation.

model analysis of patch antennas [6]. Particularly, when the resistance on the patch edge is very large, the current is blocked on the patch edge, the accumulation of charges on the patch edge results in high fringing electric fields here which contain y-directed components. The resistance on the patch edge of a rectangular patch antenna is determined by two factors: resonance and patch width which are discussed respectively as follows.

A. Resonance

As stated by Balanis [6], the maximum resistance of patch antenna appears on the edge of the patch at its resonant frequency. (2) is shown here to describe the physical parameters of rectangular patch antenna at resonance [6].

$$L = \frac{c}{2f_r\sqrt{\epsilon_{reff}}} - 2h \times 0.412 \frac{(\epsilon_{reff}+0.3)(\frac{W}{h}+0.264)}{(\epsilon_{reff}-0.258)(\frac{W}{h}+0.8)} \quad (2)$$

where c the free space velocity of light, f_r is the resonant frequency and ϵ_{reff} is the effective permittivity, which is expressed in (3).

$$\epsilon_{reff} = \frac{\epsilon_r+1}{2} + \frac{\epsilon_r-1}{2}[1+12\frac{h}{W}]^{-1/2} \quad (3)$$

(2) demonstrates that the resonance of a rectangular patch antenna is related to the patch length L, width W, dielectric thickness h and the dielectric constant ϵ_r.

B. Patch Width

The resonant input resistance on the patch edge is expressed as follows [6].

$$R_{in} = \frac{1}{2(G_1 \pm G_{12})} \quad (4)$$

where G_1 is the self-conductance at the one edge of patch antenna, G_{12} is the mutual conductance between the two edges. The expression of G_1 and G_{12} can also be found in [6], which are listed below.

$$G_1 = \frac{1}{\pi\eta}\int_0^{\pi}[\frac{\sin(\frac{k_0W}{2}\cos\theta)}{\cos\theta}]^2 \sin^3\theta d\theta \quad (5)$$

$$G_{12} = \frac{1}{\eta\pi}\int_0^{\pi}[\frac{\sin(\frac{k_0W}{2}\cos\theta)}{\cos\theta}]^2 J_0(k_0L\sin\theta)\sin^3\theta d\theta \quad (6)$$

In (5) and (6), $k_0 = \frac{2\pi}{\lambda_0}$, the wave number in the free space and λ_0 is the wavelength in free space at the resonant frequency, η is the characteristic impedance in free space.

The above equations illustrate that the patch width is inversely proportional to the resonant input resistance on the patch edge, hence also inversely proportional to the y-directed electric fields there.

In conclusion of this section, the high electric fields or y-directed electric fields on the patch edge are preferably obtained at resonance of a patch antenna with a narrow patch. This property is also examined by simulation software HFSS and shown in Figure 4(a). The patch antenna is driven from a source of available source power 1W.

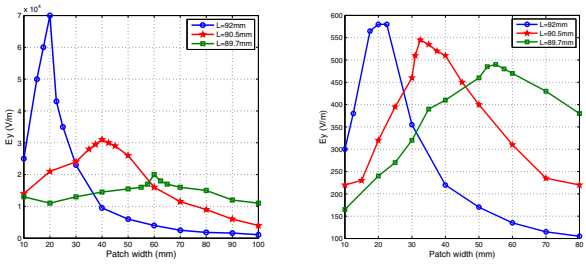

(a) Patch antenna (b) Slitted decoupler

Fig. 4. The y-directed electric fields as a function of the patch width at various patch length. The thickness of dielectric layer h=1mm, E_y is the magnitude of the r.m.s. phasors of the y-directed electric fields on the patch edge of patch antenna for sub-figure(a) and in the slit of slitted decoupler for sub-figure(b). For sub-figure(b), the width of slit s=0.5mm.

IV. Slitted Decoupler Analysis

As is assumed at the end of Section II the slitted decoupler has resonant properties similar to those of the rectangular patch antennas. The high y-directed electric fields are expected to be found in the slit at resonance of a decoupler with narrow patches. The size of a patch antenna at resonance can be made use of obtaining the size of the decoupler at resonance.

The y-directed electric fields in the slit as a function of the patch width at various patch length are obtained by HFSS and shown in Figure 4(b). In order to isolate the influence of other parameters, those parameters, including the slit width and the thickness of the dielectric layer, are held constant and the details are given in the caption of Figure 4.

By comparing Figure 4(a) and Figure 4(b), it is found that the y-directed electric fields in Figure 4(a) are neither in the same order of magnitude nor proportional to the corresponding y-directed electric fields in Figure 4(b). This enormous difference is caused by the different excitation modes. The values in Figure 4(a) are obtained for an antenna driven from a source of available source power 1W. In contrast, the values in Figure 4(b) are obtained by illuminating the slitted decoupler by a uniform plane wave of r.m.s. phasor 1V/m propagating along the -z axis. However a similarity is found in that the peak values of y-directed fields occur at similar patch sizes in both antenna mode and decoupler mode. The comparison tells us that the resonant properties of the slitted decoupler

are similar to those of rectangular patch antennas in terms of patch size. The new design principles in designing a slitted decoupler are so proposed that: the top patch length, width, the dielectric constant and thickness of the dielectric layer should be considered together to achieve the optimum resonance. The resonance of the slitted decoupler mainly depends on the patch length (around half wavelength after considering the effects of the dielectric material) but other mentioned parameters also play a significant role in achieving resonance. Moreover, on condition that the slitted decoupler is resonant, the high y-directed electric fields in the slit are obtained preferably by narrow patch width. This design principle is verified by the experiment in next section.

V. Experiment

Because of the limitation of material, we do not have the low loss polyester, which is used in simulation; what we have is FR4 board which thickness is 1.6mm, dielectric constant is 4.4, and loss tangent is 0.02. Based on the FR4 board, two slitted decoupler with different patch width (one narrow and the other wide) are designed by simulation software HFSS. Both of them are made to be resonant at 923MHz, which is the center of the Australian UHF RFID frequency band, by adjusting the patch length. The two fabricated decouplers are shown in Figure 5.

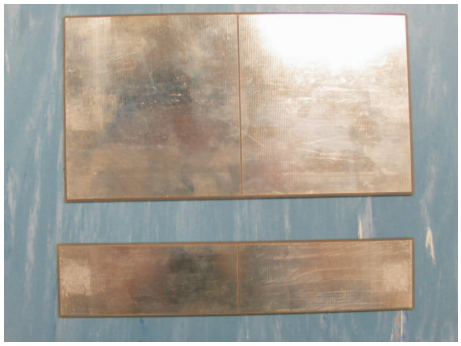

Fig. 5. The fabricated decouplers. The size of each patch of the narrow decoupler is 76mm(L)×30mm(W). The size of each patch of the wide decoupler is 78mm(L)×80mm(W). The slit width s is 0.5mm in both cases.

Two commercial tags are selected for this experiment; both designs are based on a dipole antenna pattern. For distinguishing them, they are marked by the name "Tag1" and "Tag2". The overall size of the two tags is around 90mm×25mm. The tested reading ranges of the tags in different situations are shown in Table I. In Table I, the number in the top row presents the different testing situations. In detail, the different meanings of these numbers are listed as follows.

"1": The testing tag is put in free space. "2": The testing tag is put above a large ground plane at a distance 0.1mm. "3": The testing tag is put above the narrow decoupler at a distance 0.1mm. "4": The testing tag is put above the wide decoupler at a distance 0.1mm. "5": The testing tag is put above a large ground plane at a distance 6.5mm. "6": The testing tag is put above the narrow decoupler at a distance 6.5mm. "7": The testing tag is put above the wide decoupler at a distance 6.5mm.

The reading range is tested under the Australian regulations on UHF RFID systems. In detail, the frequency band is from 920MHz to 926MHz and the maximum radiated power is 4W EIRP (Equivalent isotropically radiated power).

TABLE I
READING RANGE OF TWO TAGS IN DIFFERENT SITUATIONS.

Tags	1	2	3	4	5	6	7
Tag1	2.48m	0m	0.53m	0.43m	0.31m	0.85m	0.70m
Tag2	2.63m	0m	0.51m	0.38m	0.42m	1.67m	1.3m

By comparing the reading ranges among Columns 2, 3, 4 and among Columns 5, 6, 7 it is found that the tag on the decoupler performs much better than the tag on the ground plane, which illustrates that the decoupler does help the tag to be detected on metal. Moreover, it is found that the tag on the narrow decoupler works better than that on the wide decoupler, which complies with the conclusion made in Section IV. By comparing the reading ranges between Columns 3, 6 and between Columns 4, 7, it is found that the tag works better when it is put further away from the decoupler than that when it is put in close proximity of the decoupler.

VI. Conclusion

A conclusion is drawn that the slitted decoupler proposed by Brown et al. [5] does solve the problem for detecting metallic items in UHF RFID systems. The slitted decoupler is equipped with significant advantages, such as low profile and simple structure, compared with other solutions. However, some design principles proposed in [5] are not correct according to the analysis in this paper; as a result, some new principles in designing slitted decoupler are proposed. Simulation and experiment show that the new design principles can improve the performance of the slitted decoupler.

References

[1] K. Finkenzeller, *RFID handbook: fundamentals and applications in contactless smart cards and identification*, 2nd ed. John Wiley and Sons, 2003.

[2] Sung-Soo Kim, Yeo-Choon Yoon, and Ki-Ho Kim, "Electromagnetic wave absorbing properties of high-permittivity ferroelectrics coated with ITO thin films of 377 Omega," *Journal of Electroceramics*, vol. 10, no. 2, pp. 95–101, 05 2003.

[3] D. Sievenpiper, Lijun Zhang, R. Broas, N. Alexopolous, and E. Yablonovitch, "High-impedance electromagnetic surfaces with a forbidden frequency band," *IEEE Transactions on Microwave Theory and Techniques*, vol. 47, no. 11, pp. 2059–74, 11 1999.

[4] J. McVay, N. Engheta, and A. Hoorfar, "High impedance metamaterial surfaces using hilbert-curve inclusions," *Microwave and Wireless Components Letters, IEEE*, vol. 14, no. 3, pp. 130–132, March 2004.

[5] R. BROWN, James, R. LAWRENCE, Christopher, R. CLARKE, Paul, and N. DAMERELL, William, "Electromagnetic radiation decoupler," Great Britain Patent publication WO/2007/000 578, June 22, 2006.

[6] C. A. Balanis, *Antenna Theory*, 3rd ed. Hoboken, New Jersey: John Wiley, 2005.